ORGANOMETALLICS

ARTICLE

pubs.acs.org/Organometallics

Iron and Cobalt Complexes of 2,3,7,8-Tetrahydroacridine-4,-5(1*H*,6*H*)-diimine Sterically Modulated by Substituted Aryl Rings for the Selective Oligomerization to Polymerization of Ethylene

Vinu Krishnan Appukuttan,[†] Yinshan Liu,[†] Bong Chul Son,[†] Chang-Sik Ha,[†] Hongsuk Suh,[‡] and Il Kim*[,†]

[†]The WCU Center for Synthetic Polymer Bioconjugate Hybrid Materials, Department of Polymer Science and Engineering, Pusan National University, Busan 609-735, Korea

[‡]Department of Chemistry and Chemistry Institute for Functional Materials, Pusan National University, Pusan 609-735, Korea

Supporting Information

ABSTRACT: A new series of Fe(II) and Co(II) complexes of sterically modulated 2,3,7,8-tetrahydroacridine-4,5(1*H*,6*H*)-diimine by substituted aryl rings are synthesized. The complex synthesis is achieved through a one-pot methodology by reacting one equivalent of 2,3,7,8-tetrahydroacridine-4,5(1*H*,6*H*)-dione with two equivalents of required aniline derivatives together with Fe or Co salt in boiling acetic acid. The single-crystal X-ray analyses of Fe and Co complexes bearing a 2,6-diisopropyl-substituted ligand, (*N*,*N*′*E*,*N*,*N*′*E*)-*N*,*N*′-(2,3,7,8-tetrahydroacridine-4,5-(1*H*,6*H*)-diylidene)bis(2,6-diisopropylaniline), show a distorted trigonal-bipyramidal geometry for the metal center, a deviation from square-pyramidal geometry due to the opening up of the coordination sphere originating from structural rigidity of the carbonyl carbon atom achieved through cyclization. All the complexes show high activity toward ethylene activation when treated with methylaluminoxane as a cocatalyst. The *ortho* substituents of the aryl rings and the type of metal have a significant effect on ethylene activation and specifically on product distribution. The Fe complex with a 2,6-diisopropyl-substituted bis(imino)tetrahydroacridyl ligand produced polyethylene of moderate molecular weight (18 000). On changing the *ortho* substitution of the ligand from 2,6-diisopropyl to 2,6-dimethyl, the Co complexes produce polyethylene waxes and oligomers of predominantly α-olefins simultaneously, obeying Schulz−Flory distribution. The Co complexes bearing ligands with less sterically hindered substituents at the *ortho* position behave exclusively as dimerization catalysts.

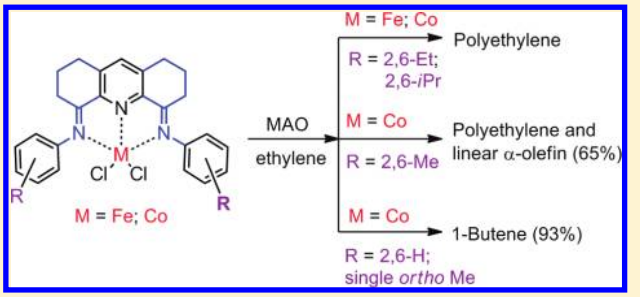

INTRODUCTION

The market for polyolefins and α-olefins is in the tens of billions of dollars, both indicating their importance and stimulating interest in academic and industrial research in this field. Polyolefins, with an annual market of over 110 million tons, are half the volume of all synthesized plastics.[1] α-Olefins have been extensively used as substrates for preparing detergents, lubricants, plasticizers, and oil field chemicals or as monomers for copolymers, etc. Originally linear α-olefins (LAOs) were produced by the Ziegler (Alfen) process, which consists in a controlled oligomerization of ethylene in the presence of $AlEt_3$ at 90−120 °C at a monomer pressure of 100 bar.[2−4] Driven by academic and industrial considerations of the important process of ethylene oligomerization for α-olefins, efficient catalysts and catalytic processes are pursued for high catalytic activity and selectivity for the formation of linear α-olefins. Over the past decade, progress has been made in ethylene reactivity (polymerization and oligomerization) by late transition metal complex catalysts.[5−9] The Fe and Co systems derived from 2,6-bis(imino) pyridines, initially discovered by the groups of Brookhart and Gibson individually, are well known.[10−14] There are many works on modifying 2,6-bis(imino)pyridyl metal complexes.[5−8,14−16] However, only few reports showed alternative models for Fe and Co catalysts with catalytic activity from moderate to high.[17−19]

Gibson replaced the pyridine ring by a pryimidine one, resulting in a somewhat less active catalyst.[20] Bisimines derived from hydrazines or 1-amino pyrroles instead of anilines were also found to be efficient in ethylene activation.[21] Apart from the works on derivatizations of 2,6-bis(imino)pyridyl metal complexes, there have been a lot of reports based on alternative models of catalysts for ethylene reactivity through designing novel organic compounds as ligands with tridentate N^N^N coordination features such as 2-imino-1,10-phenanthrolines,[22] 2-(benzimidazol-2-yl)-1,10-phenanthrolines,[23] 2-oxazoline-1,10-phenanthrolines,[24] 2-quinoxalinyl-6-iminopyridines,[25] 2-(benzimidazolyl)-6-iminopyridines,[26] *N*-((pyridin-2-yl)methylene)quinolin-8-amine,[27] 2-methyl-2,4-bis(6-iminopyridin-2-yl)-1*H*-1,5-benzodiazepines,[28] *N*-picolylethylenediamines,[29] 6-(organyl)-2-(imino)pyridines,[30] 2-(1*H*-2-benzimidazolyl)-6-(1-(arylimino)ethyl)pyridines,[31] and 2,8-bis(1-aryliminoethyl)-

Received: January 22, 2011
Published: March 24, 2011

   dx.doi.org/10.1021/om2000629 | *Organometallics* 2011, 30, 2285–2294

Scheme 1. Synthesis of Fe and Co Complexes

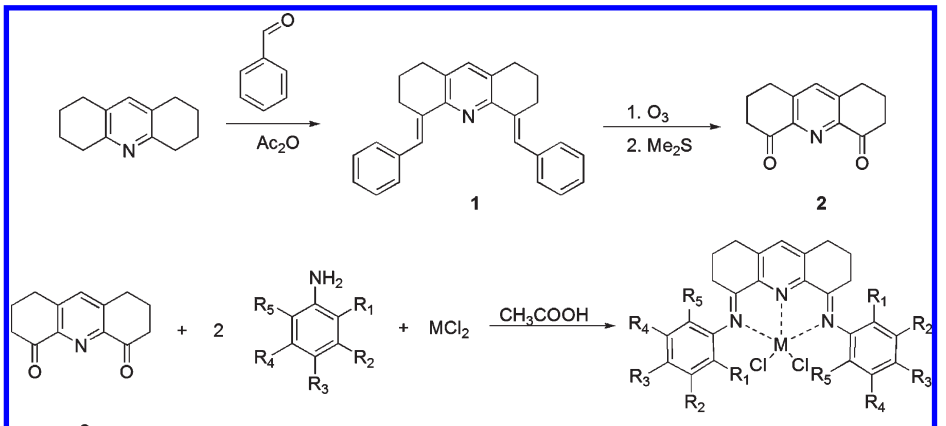

	M	R_1	R_2	R_3	R_4	R_5
3	Fe	Me	H	H	H	Me
4	Fe	Et	H	H	H	Et
5	Fe	*i*-Pr	H	H	H	*i*-Pr
6	Fe	Me	H	Me	H	Me
7	Fe	H	H	H	H	H
8	Co	Me	H	H	H	Me
9	Co	Et	H	H	H	Et
10	Co	*i*-Pr	H	H	H	*i*-Pr
11	Co	Me	H	Me	H	Me
12	Co	H	H	H	H	H
13	Co	Me	Me	H	H	H
14	Co	Me	H	Me	H	H
15	Co	Me	H	H	Me	H
16	Co	H	Me	H	Me	H

quinolines.[32] In general, Fe and Co complexes not only show high catalytic activities but also produce oligomers and polyethylenes (PEs) of high linearity with terminal vinyl groups.[31]

Initial studies involving 2,6-bis(imino)pyridines of Fe and Co have shown that ketimines are relatively more active than aldimines.[13] Also these catalysts have shown a significant stereoelectronic effect of N-aryl substituents toward ethylene activation especially in determining the polymer microstructure.[16] The 2,6-diisoproyl-substituted complexes produce strictly linear polyethylene polymer with high molecular weight (MW), and the MW decreases as the *ortho* substituents are changed to methyl through ethyl.[10] It was quite interesting to observe that the introduction of only one *ortho* substituent to iron-based complexes resulted in the production of linear alpha olefins over polymer.[12] Simultaneous formation of both polyethylene and linear alpha olefins obeying a Schulz−Flory distribution resulted when a C_1-symmetric 2,6-bis(arylimino)pyridyl iron dichloride precursor was employed.[33] Iron complexes of halogen-substituted 2,6-bis(imino)pyridyl ligands were also found to produce polymer with simultaneous production of linear alpha olefins, while their cobalt analogues were totally inactive toward ethylene.[11] Beyond such modifications to the ligand aryl substituents and central donor moiety, there have been only very few attempts to verify the effect of changes to the substituents at the imine carbon atoms. Esteruelas reported a chromium-based ethylene polymerization catalyst having a phenyl group as backbone substituent.[34] Smit and co-workers have shown the dramatic effect of ether and thioether backbone substituents for the polymerization of ethylene.[35] The bulky phenoxides or thioether derivatives afford high activities, while the methoxy derivative was inactive.

In this context, in the present work, we are attempting to modify the central pyridine donor by replacing that with a 2,3,7,8-tetrahydroacridine-4,5(1*H*,6*H*)-diimine by using a 2,3,7,8-tetrahydroacridine-4,5(1*H*,6*H*)-dione as a carbonyl source for the bisimine ligand. The dione compound is combined with two equivalents of required aniline derivatives and then with Fe or Co salt in a one-pot methodology to give a series of coordination complexes. The linking of the aldimine group to the pyridyl ring through cyclization could bring structural rigidity to the bisimino ligand framework, reducing the flexibility along the imine bond connecting the pyridyl and aryl rings. Under this circumstance, in order to investigate the effect of number, nature, and position of the substituents on the aryl rings toward the catalytic activity, complexes with different N-aryl substitution are employed. All the complexes are characterized for their mass and elemental composition, and the molecular structure was elucidated by single-crystal X-ray analysis for a few complexes. The complexes are extensively studied for their ethylene polymerization/oligomerization activity with complete characterization of polymers and oligomers.

RESULTS AND DISCUSSION

Synthesis and Structure of Complexes. The procedures for the synthesis of complexes are summarized in Scheme 1. The dione compound **2** derived from a 2,3:5,6-dicycloalkeno pyridine moiety was synthesized according to a previous report.[36]

dx.doi.org/10.1021/om2000629 |*Organometallics* 2011, 30, 2285–2294

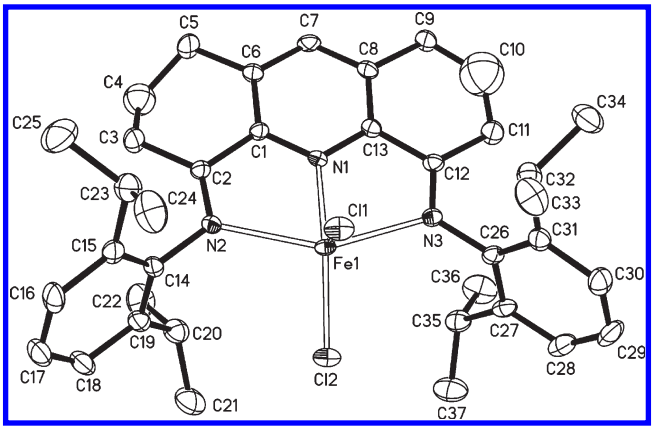

Figure 1. ORTEP representation of complex **5** with 50% thermal ellipsoids. Hydrogen atoms are omitted for clarity. Selected bond lengths [Å] and angles [deg]: Fe(1)−N(1) 2.087(4), Fe(1)−N(2) 2.313(4), Fe(1)−N(3) 2.320(4), Fe(1)−Cl(1) 2.2851(13), Fe(1)−Cl(2) 2.2429(13), C(2)−C-(3) 1.516(6), C(3)-C4) 1.481(9), C(4)−C(5) 1.532(9), C(12)−C(11) 1.518(6), C(11)−C(10) 1.376(14), C(10)−C(9) 1.406(13); N(1)−Fe-(1)−N(2) 73.22(13), N(1)−Fe(1)−N(3) 73.01(13), N(2)−Fe(1)−N(3) 145.78(13), N(1)−Fe(1)−Cl(1) 111.32(10), N(2)−Fe(1)−Cl(1) 99.83(10), N(3)−Fe(1)−Cl(1) 97.34(9), N(1)−Fe(1)−Cl(2) 139.20(10), N(2)−Fe(1)−Cl(2) 100.92(10), N(3)−Fe(1)−Cl(2) 100.9(10), C(2)−C(3)−C(4) 112.8(5), C(3)−C(4)−C(5) 112.4(6), C(12)−C(11)−C(10) 115.0(7), C(11)−C(10)−C(9) 131.2(11).

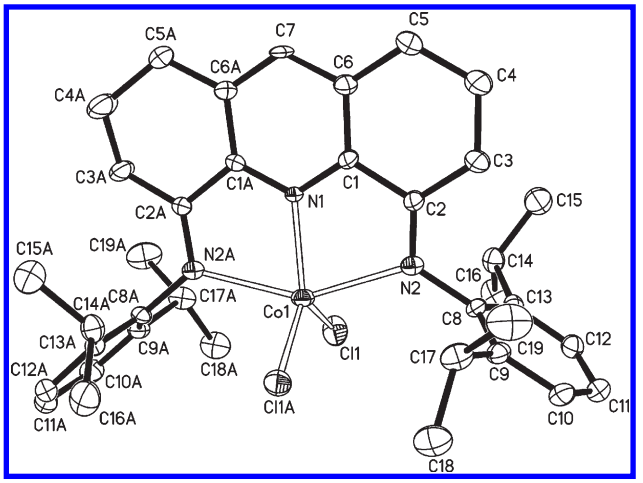

Figure 2. ORTEP representation of complex **10** with 50% thermal ellipsoids. Hydrogen atoms are omitted for clarity. Selected bond lengths [Å] and angles [deg]: Co(1)−N(1) 2.037(4), Co(1)−N(2) 2.301(4), Co(1)−Cl(1) 2.2383(14), C(2)−C(3) 1.490(6), C(3)−C4) 1.499(7), C(4)−C(5) 1.492(8); N(1)−Co(1)−N(2) 75.08(9), N(2)−Co(1)−N-(2A) 150.16(18), N(1)−Co(1)−Cl(1) 121.10(5), N(2)−Co(1)−Cl(1) 97.59(10), C(2)−C(3)−C(4) 113.0(5), C(3)−C(4)−C(5) 113.2(6).

In order to avoid a complex purification procedure and to maximize the yield, a one-pot methodology is employed for the synthesis of complexes based on previous reports.[27,37,38] The reaction is performed in boiling acetic acid for 8 h by taking stoichiometric amounts of diketone, corresponding aniline, and metal chlorides. Along with the condensation of the diketone and the amines, the central metal atom is incorporated to the ligands to give the desired complexes. The complexes were precipitated in diethyl ether and filtered, dissolved in CH_2Cl_2, reprecipitated in diethyl ether, separated, and dried to get pure complexes. All the complexes **3**−**15** were synthesized in good yields and were air-stable. The isopropyl derivatives of Fe and Co complexes **5** and **10** were characterized by single-crystal X-ray crystallography.

Crystals of complexes **5** and **10** suitable for X-ray crystallography were grown by slow diffusion of diethyl ether into a solution of complexes in CH_2Cl_2. The molecular structures and selected bond lengths and angles of the isopropyl derivatives of iron (**5**) and cobalt complexes (**10**) are shown in Figures 1 and 2, respectively. The metal center of both complexes is isostructural, having distorted trigonal-bipyramidal geometry. The basal plane is formed by the acridyl N atom and the two chloride atoms, while the two imino N atoms occupy the apical position. The essential difference between the two complexes arises from the variation of the structural orientation of the ligand backbone. The cobalt complex, **10**, possesses a C_2 axis passing through C(7)−N(1)−Co(1) and a inversion plane ($i_{\sigma h}$) passing through C(7)−N(1)−Co(1), making a symmetrical spatial orientation of the atoms along the plane with identical bond lengths and angles. Thus the two symmetry elements give **10** a near C_{2h} point group. The two cyclic rings on the pyridine show a single-bond character with bond distances ranging from 1.490(6) to 1.499(7) Å and bond angles in the range 113.0(5)−113.2(6)°. Since the sp^3-hybridized C(4) is bonded to two adjacent sp^3 carbon atoms (C(2) and C(5)), in order to attain a near-tetrahedral orientation, C(4) is positioned away from the pyridyl plane. In the case of complex **5**, there is single-bond character in one ring containing C(2), C(3), C(4), and C(5), with distances in the range 1.481(9)−1.532(9) Å and angles 112.4(6)−112.8°, while for the other ring the C(11)−C(10) bond shows a double-bond character (1.376(14) Å) and C(10)−C(9) a partial double-bond character (1.406(13) Å), making angles of 115.0(7)° and 131.2(11)° between them. This might be an aberration rather than a structural feature originating from the estimation of position of the atoms due to the low quality of the microcrystal. The existence of a nonsymmetric atomic orientation causes complex **5** to have a C_1 point group.

For both complexes, the M−N (acridyl) bond length is significantly shorter (2.087(4) Å for **5** and 2.037(4) Å for **10**) than the M−N (imino) bond (varying from 2.301(4) to 2.320(4) Å). Comparing the complexes **5** and **10** with the well-known bisiminopyridyl Fe and Co complexes, where the M−N (pyridyl) bond is 2.088(4) Å for Fe and 2.051(3) Å for Co, it could be seen that the metal is more closely placed to the acridyl N atom in the present system. On the other hand for the present complexes the M−N (imino) bond was found to be significantly longer than the bisiminopyridyl complexes, where the distances between the two M−N (imino) bonds for Fe are 2.238 and 2.50 Å, respectively, and that for Co is 2.11 Å each.[10] This variation is probably due to linking the aldimino group to the pyridyl ring through cyclization. In addition the distance (4.483 Å) between the two imino N atoms of the Co complex **10** is longer than that (4.173 Å) of the Co complex bearing 2,6-bis(imino)pyridyl ligands.[13] This elongation slightly opens up the coordination sphere and thus gives a space incorporating the central metal atom within the N_3 plane. In fact the cobalt atom lies within the N_3 plane, while iron is deviated by a distance of 0.16 Å. Thus this structural variation of the ligand gives a distorted trigonal-bipyramidal geometry to the metal center, which is comparable to a square-pyramidal geometry of analogous Fe and Co complexes of 2,6-bis(imino)pyridine. The double-bond nature of the imino bond is kept intact for both complexes (ranging from 1.268(6) to 1.282(5) Å). The chloride atoms, Cl(1) and Cl(2), are bonded to

dx.doi.org/10.1021/om2000629 |*Organometallics* 2011, 30, 2285–2294

the Fe atom by a distance of 2.2852(13) and 2.2429(13) Å, respectively, for **5**, and those bonded with the Co atom are at a equidistance of 2.2383(14) Å for **10**. The phenyl rings in both complexes essentially lie orthogonal to the plane of the backbone with dihedral angles ranging from 76° to 87°.

Effect of Catalyst Structure on Ethylene Oligomerization/Polymerization. All the catalysts were examined for their ethylene oligomerization and polymerization capability employing MAO as a cocatalyst and toluene as a solvent under semibatch conditions. The effect of catalyst structure on oligomerization/polymerization behavior has been investigated by conducting the reactions with variable parameters such as cocatalyst concentration and temperature.

The polymerization rate (R_p) of ethylene under constant pressure using Fe (**3**−**6**) and Co (**8**−**11**) complexes combined with MAO ([Al]/[M] = 250; M = Fe or Co) changes markedly with time, as illustrated by the rate curves in Figure 3. The kinetic curves obtained with the Fe complexes show an induction or buildup period probably due to low solubility of the complexes, where the R_p increases to a maximum followed by a decay period during which the rate decreases gradually to the stationary state. In the case of kinetic curves obtained by the Co complexes there is almost no induction period, followed by a rapid decay. The kinetic curves show that it takes longer to form active sites from the reaction of Fe complexes with MAO in the presence of ethylene monomer than the corresponding Co complex systems.

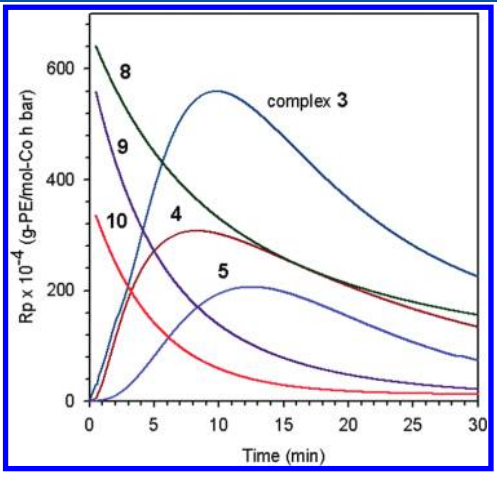

Figure 3. Ethylene polymerization rate profiles obtained by different complexes. Polymerization conditions: catalyst = 2.5 μmol, [Al]/[M] = 250 (Mt = Fe or Co), P_{C2H4} = 1.3 bar, toluene = 80 mL, T = 30 °C, and time = 30 min.

The polymerization results are also summarized in Table 1. Note that the type of metal center has a significant effect not only on the kinetic curve but also on the catalyst activity. Although the Co catalysts show a higher maximum rate of polymerization than the corresponding Fe analogues, they show a lower average rate of polymerization than the corresponding Fe analogues since the Co catalysts deactivate very rapidly. The results also show that the polymerization activity is strongly influenced by 2,6-substituents on the N-aryl ring as observed in the other catalyst system.[13] The less bulky methyl-substituted complexes are more active than the bulkier isopropyl one, and the activity of ethyl-substituted complexes lies in between (Table 1). This observation is the direct consequence of the effect of the size of the *ortho* substituents toward the insertion of monomer; bulkier substituents offer maximum resistance to incoming monomers to the active metal center. In order to determine the electronic effect of the substituents, we replaced the 4-position of the N-aryl ring by keeping the 2,6-substituents as methyl to generate the Fe complex **6** and the Co complex **11**. To our surprise both complexes showed relatively lower productivities in ethylene activation (Table 1, entries 4, 6) than those observed for 2,6-bis(imino)-tetrahydroacridine catalysts, **3** and **8**, demonstrating that the electron-donating methyl groups on the 4-position of the N-aryl ring probably have a negative effect on the catalytic activity.

The steric bulk offered by *ortho* imino-aryl sustituents has a significant influence on the polymer properties and has been a subject of many investigations. Bulky *ortho* substituents usually result in high molecular weight polymers, and the MW usually depends on the size of those substituents. Brookhart and co-workers demonstrated that 2,6-isopropyl-substituted complex produced PE with the highest MW, and as the 2,6-substituent was changed to ethyl and methyl, the MW also decreased accordingly.[13] The introduction of only one *ortho* substituent on the aryl ring resulted in oligomerization producing α-olefins. For the C_s and C_1 symmetric bis(imino)pyridyl complexes of Fe and Co containing one alkyl-imine and one aryl-imine, Bianchini and co-workers found the formation of ethylene oligomers with high selectivity for α-olefins.[15] The significant influence of the slight variation of the bulkiness of the 2,6-arylimino substituent on the product microstructure was established by Qian and co-workers utilizing halogens as *ortho* aryl groups.[39] The Fe complex

Table 1. Results of Ethylene Polymerization with Various Fe and Co Catalysts[a]

entry	cat.	$R_{p,max} \times 10^{-6}$[b]	$R_{p,av} \times 10^{-6}$[b]	M_n[c] (g/mol)	PDI[c]	oligomer[d] (%)	K[e]	T_m[f] (°C)
1	**3**	5.60	3.71	7700	3.6			131.9
2	**4**	3.08	2.17	8300	4.6			136.9
3	**5**	2.06	1.29	18 000	7.2			138.2
4	**6**	4.11	2.92	7200	6.4			132.1
5	**8**	6.42	2.98	640[g]	1.4	63.6	0.88	
6	**9**	5.59	1.33	1000	1.6			120.1
7	**10**	3.36	0.66	5200	6.6			137.8
8	**11**	5.15	2.54	620[g]	1.5	63.5	0.88	

[a] Polymerization conditions: catalyst = 2.5 μmol, cocatalyst = MAO, [Al]/[M] = 250, P_{C2H4} = 1.3 bar, toluene = 80 mL, and time = 30 min. [b] The maximum rate of polymerization ($R_{p,max}$) and the average rate of polymerization over 30 min ($R_{p,av}$) in (g-product)·(mol-metal)$^{-1}$·h^{-1}·bar^{-1}. [c] Number average molecular weight (M_n) and polydispersity index (PDI) determined by GPC. [d] From methanol-soluble fraction. [e] Schulz−Flory distribution constant, K = (moles of C_{14})/(moles of C_{12}). [f] Determined by DSC. [g] From methanol-insoluble portion.

dx.doi.org/10.1021/om2000629 |*Organometallics* 2011, 30, 2285–2294

Table 2. Results of Ethylene Polymerization with Complex 5 at Different Reaction Conditions[a]

entry	catalyst (μmol)	[Al]/[Fe]	T_p (°C)	yield (g)	$R_{p,av} \times 10^{-6}$ [b]	M_n [c] (g/mol)	M_w/M_n [c]	T_m [d] (°C)
1	2.5	50	30	0.34	0.21	49 800	3.9	141.9
2	2.5	100	30	0.52	0.32	32 500	6.2	141.1
3	2.5	250	30	2.52	1.55	18 000	7.2	138.2
4	2.5	500	30	2.05	1.26	5800	21.1	132.8
5	2.5	1000	30	1.79	1.10	2100	42.0	131.5
6	2.5	2000	30	1.20	0.74	1100	19.9	127.9
7	5	500	30	7.15	2.20	2800	27.5	131.6
8	5	500	50	5.40	1.66	1700	7.0	129.9
9	5	500	70	4.94	1.52	1600	2.0	127.6

[a] Polymerization conditions: P_{C2H4} = 1.3 bar, toluene = 80 mL, and time = 30 min. [b] The average rate of polymerization over 30 min ($R_{p,av}$) in (g-PE)·(mol-Fe)$^{-1}$·h^{-1}·bar^{-1}. [c] Determined by GPC. [d] Determined by DSC.

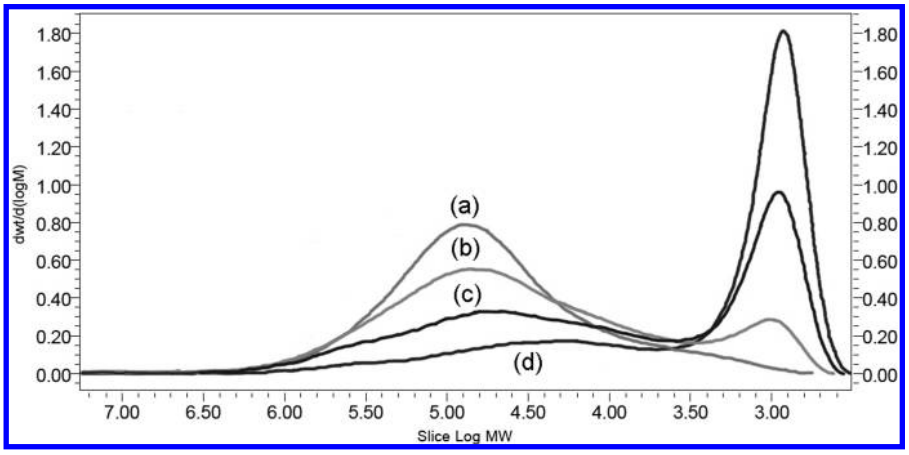

Figure 4. GPC curves of polyethylene samples obtained by complex **5** at different [MAO]/[**5**] ratios: (a) 250, (b) 500, (c) 1000, and (d) 2000. Polymerization conditions: catalyst = 2.5 μmol, P_{C2H4} = 1.3 bar, toluene = 80 mL, T = 30 °C, and time = 30 min.

having the larger bromide groups as 2,6-substituent produced PEs with high MW (101 000), while the Fe complex with smaller chloride groups yielded PEs with lower MW by 10-fold, and finally the Fe complex substituted by fluoride groups produced LAOs with a K value (Schulz−Flory constant for oligomer distribution) of 0.7 under identical reaction conditions. On the contrary, the *meta* and *para* substituents on the aryl rings had only an electronic effect on the polymerization, the product distribution remaining similar.

For the present catalytic system, all the polymers were characterized by moderate to low MW with broad distribution, which is generally associated with bisimino complexes of Fe and Co.[13] The Fe complexes with the 2,6-dimethyl (**3**) and 2,4,6-trimethyl (**6**) substituted bis(imino)tetrahydroacridyl ligand produced linear PE with the number average molecular weight (M_n) of 7700 and 7200, respectively, while the Fe complex with a 2,6-diisopropyl-substituted bis(imino)tetrahydroacridyl ligand yielded PE with an M_n of 18 000. A similar steric effect on the product distribution was also observed for the Co complexes, even though the Co complexes produce PEs with lower MW than Fe homologues. Thus, complexes **8** and **10** produce PEs with M_n's of 640 and 5800, respectively. Note that complex **8** also produces LAO together with low MW PE (Table 1, entry 5). The product analysis reveals that the LAO content is 63.6 wt % of the total product with a distribution that closely resembles Schulz−Flory rules, having a K value of 0.89.[40−44] Complex **11** shows similar product distribution to complex **8** (Table 1, entry 8). Detailed simultaneous oligo- and polymerizations by using complex **8** will be discussed later.

All the polymers were found to be highly linear according to the microstructural analysis by NMR spectroscopy. A slightly higher melting temperature (T_m) values are observed for Fe complexes than their Co analogues. The PE produced by **5** shows a T_m of 138.2 °C and that by **3** shows a T_m of 131.9 °C. For Co complexes, **10** produce PEs with a T_m of 137.8 and **9** produces waxes melting at 120.1 °C, respectively. High T_m values for isopropyl derivatives are due to the strictly linear nature of the polymer coupled with high MW.

Effect of Reaction Conditions on Ethylene Polymerization. The effect of MAO concentration and temperature on the polymerization behavior has been investigated by using complex **5** as a representative catalyst, and the results are summarized in Table 2. The polymerizations conducted at different MAO concentrations ([Al]/[Fe] = 50−2000) show that the catalytic activity increases from an [Al]/[Fe] ratio of 50 to 250 and then starts to decrease at higher ratios (Table 2, entries 1−6). Complex **5** combined with a low [Al]/[Fe] ratio of 50 produces PE with higher MW (M_n = 49 800); however, the M_n value decreases to 1100 at a high [Al]/[Fe] ratio of 2000, due to the facilitated chain transfer to aluminum. The GPC trace is monomodal in nature for [Al]/[Fe] = 50, and the characteristic bimodal nature of Fe catalysts started to

dx.doi.org/10.1021/om2000629 |*Organometallics* 2011, 30, 2285–2294

Table 3. Simultaneous Oligo- and Polymerizations of Ethylene[a]

entry	catalyst	[Al]/[Co]	T_p (°C)	activity kg/mol$_{Co}$·h·bar	total yield (g)	oligomer yield (%)	% α-olefin[b]	α[c]	β
1	**8**	250	30	4093	7.97	63.6	99>	0.88	0.14
2	**8**	500	30	4936	8.02	63.9	99>	0.91	0.10
3	**8**	1000	30	5742	9.33	64.2	99>	0.91	0.10
4	**8**	2000	30	5096	8.28	65.3	95	0.89	0.12
5	**8**	1000	50	3882	7.56	65.9	98	0.90	0.11
6	**8**	1000	70	1022	1.66	70.2	97	0.87	0.15
7	**8**[d]	1100	30	9316	2.02	78.3	90	0.88	0.14
8	**7**	250	30	575	1.12	99>	99>	0.50	1.00

[a] Polymerization conditions: P_{C2H4} = 1.3 bar, toluene = 80 mL, and time = 30 min. [b] Determined by GC. [c] Schulz−Flory distribution constant, K = (moles of C_{14})/(moles of C_{12}). [d] Conditions: cocatalyst =100 MAO + 1000TMA, time = 10 min.

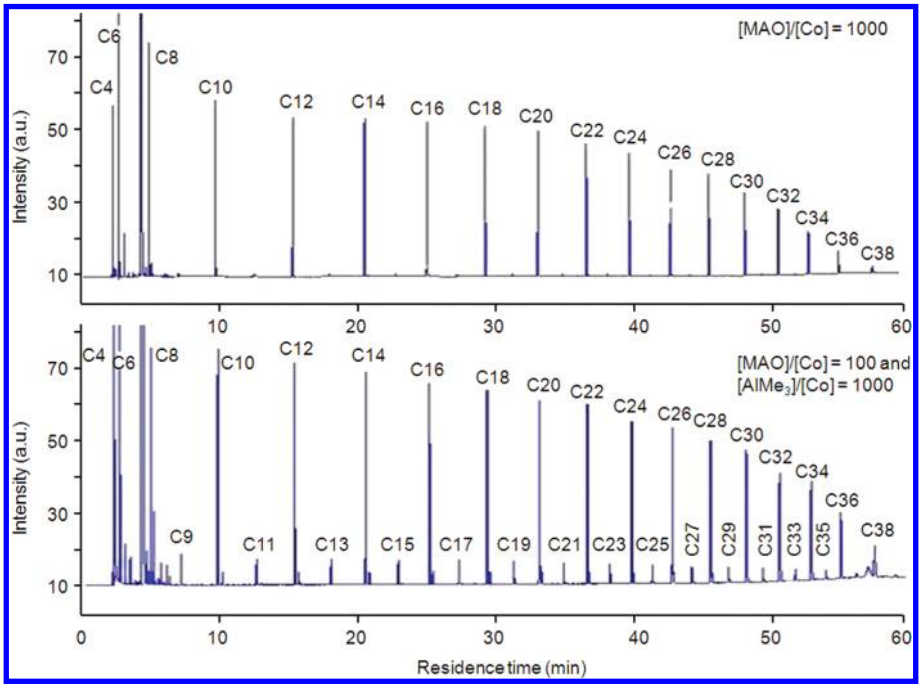

Figure 5. GC traces of ethylene oligomers obtained by complex **8** at polymerization conditions of catalyst = 2.5 μmol, P_{C2H4} = 1.3 bar, toluene = 80 mL, T = 30 °C, time = 30 min, and (top) [MAO]/[Co] = 1000 and (bottom) [MAO]/AlMe$_3$]/[Co] = 100/1000/1.

appear from [Al]/[Fe] ≥ 250; hence a broadening of MWD is observed. The GPC curves of PEs produced at [Al]/[Fe] ratios 250−2000 are illustrated in Figure 4. At [Al]/[Fe] ratios of 500 and 1000, bimodal distributions can be clearly observed, and at the [Al]/[Fe] ratio of 2000 the high MW fraction almost disappeared. The formation of a low MW fraction is evidently due to the chain transfer to aluminum.[11,12]

The effect of temperature was also investigated between 30 and 70 °C (Table 2, entries 7−9). The catalytic activity decreases monotonically as the temperature increases. The R_p value decreases from 2.20 × 10^6 (g-PE)·(mol-Fe)$^{-1}$·h^{-1}·bar^{-1} at 30 °C to 1.52 × 10^6 (g-PE)·(mol-Fe)$^{-1}$·h^{-1}·bar^{-1} at 70 °C, a drop of activity about 31%. The typical Fe(II) catalyst based on tridentate pyridine bis-imine ligand [(2,6-C_6H_3(i-Pr)$_2$N=C(Me))$_2C_5H_3N$]$FeCl_2$ showed a much more severe decrease of activity, by about 90%, in the same temperature range.[10] The MW of PE decreases as the polymerization temperature increases due to the facilitated chain-transfer reactions at elevated temperatures. Note that the decrease of the MW value according to polymerization temperature is smaller than that induced by the variation of MAO concentration, demonstrating that chain transfer to aluminum is a major transfer reaction and a viable route for the formation of low molecular weight materials. The PEs produced by **5** catalysts usually have high T_m values owing to their linear structure. The polymer produced at [Al]/[Fe] = 50 has a high T_m value of 141.9 °C. As the ratio increases, T_m decreases, reaching a low value of 127.9 °C at 2000 ratio, due to the decrease in MW and broadening of its distribution.

Simultaneous Oligo- and Polymerizations of Ethylene. The simultaneous oligomerization and polymerization behavior has been investigated by using complex **8** at various conditions, since complex **8** was found to produce both waxy PE and LAOs ranging from C_4 to C_{38} in the presence of MAO. The LAO percentage ranges between 63.6% and 70.2%, as summarized in Table 3. Complex **8** gives a Schulz−Flory distribution of LAOs, which can be quantified by the α value. The α value represents the probability of chain propagation and is experimentally determined by the molar ratio of two neighboring LAO fractions,

dx.doi.org/10.1021/om2000629 |*Organometallics* 2011, 30, 2285–2294

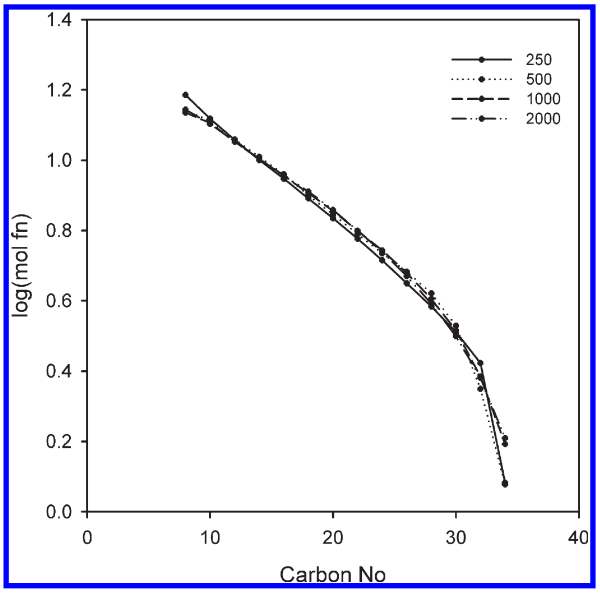

Figure 6. Molar distribution of oligomers produced by **8** at [Al]/[Co] ratios from 250 to 1000. Polymerization conditions: catalyst = 2.5 μmol, $P_{C_2H_4}$ = 1.3 bar, toluene = 80 mL, T = 30 °C, and time = 30 min.

C_{14} and C_{12} in this case [eq 1].[14]

$$\alpha = \frac{R_p}{R_p + R_{tr}} = \frac{\text{moles of } C_{n+2}}{\text{moles of } C_n} \quad (1)$$

$$\beta = \frac{R_{tr}}{R_p} = \frac{1-\alpha}{\alpha} \quad (2)$$

where R_p and R_{tr} are the rate of propagation and the rate of chain transfer, respectively. The α value ranging from 0.87 to 0.91 characteristic for the distribution of LAOs obtained with the precatalyst **8** shows that the polymerization parameters have very little effect on the LAO distribution, unlike the differences in activity, and the range encompasses the most desired values for industrial production of α-olefins.[2] Figure 5 (top) shows the typical gas chromatogram of the LAO product produced by the **8**/MAO catalyst system ([Al]/[Co] = 1000) at 30 °C. Quantitative analysis of the LAO product reveals product selectivity for linear α-olefins greater than 99%. Neither branched oligomers nor isomerization to internal olefins is observed. By adding trimethyl aluminum as a chain-transfer agent, formation of odd carbon number alkanes generated by chain transfer to aluminum was observed (Table 3, entry 7), and the gas chromatogram is shown in Figure 5 (bottom). The molar distribution of oligomers produced by the **8**/MAO system ([Al]/[Co] = 250−1000) is illustrated in Figure 6. This high selectivity, combined with a Schulz−Flory distribution, is consistent with an oligomerization mechanism starting from a cobalt alkyl species, which is generated by the reaction of **8** with MAO, followed by several insertion steps of ethylene and a chain-transfer process.

In the case of late transition metal catalyzed ethylene oligomerization, four different transfer processes can be considered: namely, β-hydrogen to metal, β-hydrogen to monomer, σ-bond metathesis, and chain transfer to Al. Since the oligomerization resulted in LAOs in excess of 99%, a Cossee-type mechanism proposed by Britovsek and co-workers based on their work on C_s symmetric Co and Fe complexes is envisaged to operate in the present system producing LAOs, with the operation of β-hydrogen transfer as the chain-transfer mechanism.[14,45] The chain transfer to aluminum cocatalyst has been detected as a minor chain-transfer mechanism; in this case odd-numbered oligomers were almost negligible [see Figure 5 (top)]. However, the odd-numbered oligomers are clearly seen by adding an excess amount of a strong transfer agent such as trimethylaluminum (TMA), due to the activated chain transfer to aluminum [see Figure 5 (bottom)]. TMA may form methyl-bridged dinuclear species that promote chain transfer. In this case, TMA acts as a separate chain-transfer agent and reduces the MW of the polymer. Although chain transfer to Al is the dominant chain-transfer mechanism at high TMA concentration, it is clear that chain transfer to Al is only a minor contribution at the general polymerization conditions employed in this study.

Table 4. Dimerization Results of Ethylene Obtained by Various Cobalt Complexes[a]

entry	catalyst	yield (g)	C_4[b] (%)	α-C_4[b] (%)
1	**12**	0.21	95.3	96.3
2	**13**	0.82	95.6	94.4
3	**14**	0.81	96.0	96.7
4	**15**	0.73	96.1	95.4
5	**16**	0.27	95.4	95.9

[a] Dimerization conditions: catalyst = 2.5 μmol, [Al]/[Co] = 250, P_{C2H4} = 1.3 bar, toluene = 80 mL, and time = 30 min. [b] Determined by GC.

Dimerization of Ethylene by Cobalt Complexes. To provide insights into ethylene activation, the present catalytic system, a cobalt complex (**12**) bearing no substituents on the aryl rings, was synthesized and tested for its activity. Surprisingly the complex produces 95.3% dimer with 96.3% selectivity to 1-butene, but the overall catalytic activity is lower than the cobalt complexes bearing ligands with 2,6-alkyl-substituted aryl rings and the iron systems (Table 4, entry 1). But a similar iron complex (**7**) produced LAOs rather than dimer with K = 0.50 (Table 3, entry 8). The cobalt complexes bearing ligands of aniline rings with unsymmetrical dimethyl substituents [2,3-dimethyl- (**13**), 2,4-dimethyl- (**14**), and 2,5-dimethyl-substituted (**15**)] and with a 3,5-dimethyl substituent (**16**) were also synthesized and tested for ethylene oligomerization. As shown in Table 4, all the catalysts were active in selective dimerization to 1-butene, with the selectivity in the range 94.4−96.7%. Catalysts show high initial activity with rapid deactivation within 10 min of reaction time, and those without any *ortho* substitution deactivated much faster. These results demonstrate that, in cobalt complexes of bisimines, 2,6-dialkyl substituents on the aryl rings are a prerequisite condition to achieve higher α-olefins and/or high MW PEs.

CONCLUSIONS

In an attempt to find new alternatives for the well-known Fe and Co catalysts bearing bis(arylimino)pyridine ligands, we modified the central pyridine donor by replacing it with a 2,3:5,6-dicyclohexano pyridine by using 2,3,7,8-tetrahydroacridine-4,5(1*H*,6*H*)-dione as a carbonyl source for the bisimine ligand. The dione compound is combined with two equivalents of required aniline derivatives and metal halides in a one-pot methodology to give a series of Fe(II) and Co(II) complexes. The use of the cyclized backbone as a ligand changes the geometry of the metal center from distorted square pyramidal

for the well-known 2,6-diisopropyl-substituted bis(imino)-pyridine Fe and Co complexes to a trigonal-bipyramidal structure, as evidenced from single-crystal X-ray analyses. All the complexes show high activity toward ethylene activation when treated with MAO as a cocatalyst. The *ortho* substitution in the aryl rings of the complexes and the type of metal had a significant effect on ethylene activation and more importantly on product microstructure. Thus, the Fe complex with a 2,6-diisopropyl-substituted bis(imino)tetrahydroacridyl ligand yielded PE with the M_n of 18 000, while the Co complexes produced PE waxes and LAO obeying Schulz−Flory distribution simultaneously, changing their compositions according to the bulk of the *ortho* disubstitution. The Co complexes without any *ortho* substitution or with only one substitution behave as exclusive dimerization catalysts with over 97% selectivity toward 1-butene, which is not common in Co catalyst systems.

EXPERIMENTAL SECTION

General Procedures and Materials. All reactions and operations were performed under a purified nitrogen atmosphere using standard glovebox and Schlenk techniques. Polymerization grade ethylene (SK Co., Korea) was purified by passing it through columns of Fisher RIDOX catalyst and molecular sieve 5 Å/13X. Toluene used as solvent for polymerizations was distilled from Na/benzophenone and stored over molecular sieves (4 Å). MAO (8.4 wt % total Al solution in toluene) was donated by LG Chemicals, Korea, and was used without purification. 1,2,3,4,5,6,7,8-Octahydroacridine was purchased from TCI Chemicals. All other reagents were purchased from Aldrich Chemical Co. and used without further purification.

Characterizations. Elemental analyses were carried out using CE Instruments/Thermo Quest Italia Flash EA 1112 series. ^{1}H NMR spectra (300 MHz) and ^{13}C NMR spectra (75 MHz) of the ligands were recorded on a Varian Gemini 2000 spectrometer. Chemical shifts are reported in parts per million relative to internal $(CH_3)_4Si$ (^{1}H, ^{13}C). ^{1}H and ^{13}C NMR spectra of polyethylene (PE) samples were taken in $C_6H_6Cl_2$ at 135 °C on a Varian Unity Plus 300 (300 and 75 MHz) spectrometer. Fast atom bombardment mass spectra (FAB-MS) of the complexes were recorded on a JEOL JMS-700 spectrometer. MW and polydispersity of PE were determined by GPC (Alliance GPCV2000, RI detector) at 150 °C column temperature in 1,2,4-trichlorobenzene using polystyrene as a standard. Thermal analysis of PE was carried out by a differential scanning calorimeter (Perkin-Elmer DSC, model Pyris 1) at 10 °C/min heating rate under a nitrogen atmosphere. Oligomerization products were analyzed by an Agilent Technologies 7890 A GC system with a J&W Scientific 30 m column with 0.25 mm inner diameter.

Synthesis of Complexes. All complexes were prepared in a similar manner by using $FeCl_2 \cdot 4H_2O$ or $CoCl_2 \cdot 6H_2O$ as a metal source. A suspension of **3** (1.00 mmol) and 2 mmol of corresponding aniline derivative with metal salt in glacial acetic acid (10 mL) was refluxed for 6 h. The complex was precipitated by adding excess diethyl ether, and the precipitate was collected by filtration and washed with 3 × 5 mL of diethyl ether. Then the collected solid was dried under vacuum to yield the complex.

*(15E)-N-((E)-4-(2,6-Dimethylphenylimino)-1,2,3,4,7,8-hexahydroacridin-5(6H)-ylidene)-2,6-dimethylbenzenamine Fe(II) Chloride (**3**).* The complex was obtained as deep brown colored crystals in 68.0% yield. Anal. Calcd for $C_{29}H_{31}Cl_2FeN_3$: C, 63.52; H, 5.70; N, 7.66. Found: C, 63.02; H, 4.35; N, 7.72. FAB-MS (m/z): 512 $[M - Cl]^+$, 476 $[M - 2Cl]^+$

*(15E)-N-((E)-4-(2,6-Diethylphenylimino)-1,2,3,4,7,8-hexahydroacridin-5(6H)-ylidene)-2,6-diethylbenzenamine Fe(II) Chloride (**4**).* The complex was obtained as brown-colored crystals in 64.0% yield. Anal. Calcd for $C_{33}H_{39}Cl_2FeN_3$: C, 65.57; H, 6.50; N, 6.95. Found: C, 65.91; H, 6.12; N, 7.05. FAB-MS (m/z): 568 $[M - Cl]^+$,533 $[M - 2Cl]^+$.

*(15E)-N-((E)-4-(2,6-Diisopropylphenylimino)-1,2,3,4,7,8-hexahydroacridin-5(6H)-ylidene)-2,6-diisopropylbenzenamine Fe(II) Chloride (**5**).* The complex was obtained as brown-colored crystals in 59.0% yield. Anal. Calcd for $C_{37}H_{47}Cl_2FeN_3$: C, 67.28; H, 7.17; N, 6.36. Found: C, 67.06; H, 7.01; N, 6.55. FAB-MS (m/z): 624 $[M - Cl]^+$, 590 $[M - 2Cl]^+$.

*(15E)-N-((E)-1,2,3,4,7,8-Hexahydro-4-(mesitylimino)acridin-5(6H)-ylidene)-2,4,6-trimethylbenzenamine Fe(II) Chloride (**6**).* The complex was obtained as brown-colored crystals in 62.0% yield. Anal. Calcd for $C_{31}H_{35}Cl_2FeN_3$: C, 64.60; H, 6.12; N, 7.29. Found: C, 64.76; H, 6.01; N, 7.35. FAB-MS (m/z): 540 $[M - Cl]^+$,504 $[M - 2Cl]^+$.

*(15E)-N-((E)-1,2,3,4,7,8-Hexahydro-4-(phenylimino)acridin-5(6H)-ylidene)benzenamine Fe(II) Chloride (**7**).* The complex was obtained as deep brown colored crystals in 71.0% yield. Anal. Calcd for $C_{25}H_{23}Cl_2FeN_3$: C, 61.00; H, 4.71; N, 8.54. Found: C, 61.30; H, 4.43; N, 8.74. FAB-MS (m/z): 456 $[M - Cl]^+$, 420 $[M - 2Cl]^+$.

*(15E)-N-((E)-4-(2,6-Dimethylphenylimino)-1,2,3,4,7,8-hexahydroacridin-5(6H)-ylidene)-2,6-dimethylbenzenamine Co(II) Chloride (**8**).* The complex was obtained as green-colored crystals in 62.0% yield. Anal. Calcd for $C_{29}H_{31}Cl_2CoN_3$: C, 63.17; H, 5.67; N, 7.62. Found: C, 63.12; H, 4.37; N, 7.84. FAB-MS (m/z): 515 $[M - Cl]^+$, 480 $[M - 2Cl]^+$.

*(15E)-N-((E)-4-(2,6-Diethylphenylimino)-1,2,3,4,7,8-hexahydroacridin-5(6H)-ylidene)-2,6-diethylbenzenamine Co(II) Chloride (**9**).* The complex was obtained as green-colored crystals in 60.0% yield. Anal. Calcd for $C_{33}H_{39}Cl_2CoN_3$: C, 65.24; H, 6.47; N, 6.92. Found: C, 65.82; H, 6.08; N, 6.95. FAB-MS (m/z): 571 $[M - Cl]^+$, 534 $[M - 2Cl]^+$.

*(15E)-N-((E)-4-(2,6-Diisopropylphenylimino)-1,2,3,4,7,8-hexahydroacridin-5(6H)-ylidene)-2,6-diisopropylbenzenamine Co(II) Chloride (**10**).* The complex was obtained as brown-colored crystals in 59.0% yield. Anal. Calcd for $C_{37}H_{47}Cl_2CoN_3$: C, 66.96; H, 7.14; N, 6.33. Found: C, 67.06; H, 7.01; N, 6.55. FAB-MS (m/z): 627$[M - Cl]^+$, 590 $[M - 2Cl]^+$.

*(15E)-N-((E)-1,2,3,4,7,8-Hexahydro-4-(mesitylimino)acridin-5(6H)-ylidene)-2,4,6-trimethylbenzenamine Co(II) Chloride (**11**).* The complex was obtained as green crystals in 56.0% yield. Anal. Calcd for $C_{31}H_{35}Cl_2CoN_3$: C, 64.25; H, 6.09; N, 7.25. Found: C, 64.73; H, 6.04; N, 7.30. FAB-MS (m/z): 543 $[M - Cl]^+$, 508 $[M - 2Cl]^+$.

*(15E)-N-((E)-1,2,3,4,7,8-Hexahydro-4-(phenylimino)acridin-5(6H)-ylidene)benzenamine Co(II) Chloride (**12**).* The complex was obtained as brown-colored crystals in 65.0% yield. Anal. Calcd for $C_{25}H_{23}Cl_2CoN_3$: C, 60.62; H, 4.68; N, 8.48. Found: C, 61.07; H, 4.55; N, 8.81. FAB-MS (m/z): 459 $[M - Cl]^+$, 424 $[M - 2Cl]^+$.

*(15E)-N-((E)-4-(2,3-Dimethylphenylimino)-1,2,3,4,7,8-hexahydroacridin-5(6H)-ylidene)-2,3-dimethylbenzenamine Co(II) Chloride (**13**).* The complex was obtained as green-colored crystals in 64.0% yield. Anal. Calcd for $C_{29}H_{31}Cl_2CoN_3$: C, 63.17; H, 5.67; N, 7.62. Found: C, 63.12; H, 5.59; N, 7.71. FAB-MS (m/z): 515 $[M - Cl]^+$, 480 $[M - 2Cl]^+$.

*(15E)-N-((E)-4-(2,4-Dimethylphenylimino)-1,2,3,4,7,8-hexahydroacridin-5(6H)-ylidene)-2,4-dimethylbenzenamine Co(II) Chloride (**14**).* The complex was obtained as green-colored crystals in 67.0% yield. Anal. Calcd for $C_{29}H_{31}Cl_2CoN_3$: C, 63.17; H, 5.67; N, 7.62. Found: C, 63.00; H, 5.48; N, 7.85. FAB-MS (m/z): 515 $[M - Cl]^+$, 480 $[M - 2Cl]^+$.

*(15E)-N-((E)-4-(2,5-Dimethylphenylimino)-1,2,3,4,7,8-hexahydroacridin-5(6H)-ylidene)-2,5-dimethylbenzenamine Co(II) Chloride (**15**).* The complex was obtained as deep brown colored crystals in 57.0% yield. Anal. Calcd for $C_{29}H_{31}Cl_2CoN_3$: C, 63.17; H, 5.67; N, 7.62. Found: C, 63.12; H, 5.75; N, 7.66. FAB-MS (m/z): 517 $[M - Cl]^+$, 480 $[M - 2Cl]^+$.

*(15E)-N-((E)-4-(3,5-Dimethylphenylimino)-1,2,3,4,7,8-hexahydroacridin-5(6H)-ylidene)-3,5-dimethylbenzenamine Co(II) Chloride (**16**).* The complex was obtained as green-colored crystals in 64.0% yield. Anal. Calcd

for $C_{29}H_{31}Cl_2CoN_3$: C, 63.17; H, 5.67; N, 7.62. Found: C, 63.09; H, 5.89; N, 7.69. FAB-MS (m/z): 515 $[M - Cl]^+$, 480 $[M - 2Cl]^+$.

Crystallographic Studies. The crystal was picked up with Paraton N oil and mounted on a Bruker SMART CCD diffractometer equipped with a graphite-monochromated Mo Kα (λ= 0.71073 Å) radiation source and a nitrogen cold stream (−100 °C). The data were corrected for Lorentz and polarization effects (SAINT), and semiempirical absorption corrections based on equivalent reflections were applied (SADABS). The structure was solved by direct methods and refined by full-matrix least-squares on F^2 (SHELXTL). All the non-hydrogen atoms were refined anisotropically, and hydrogen atoms were added to their geometrically ideal positions. The crystal data for complexes **5** and **10** have been deposited at the Cambridge Crystallographic Data Center with numbers CCDC 755418 and 755419, respectively. The data can be obtained free of charge from the Cambridge Crystallographic Data Centre through www.ccdc.cam.ac.uk/data_request/cif.

Polymerization/Oligomerization Procedure. Ethylene oligomerizations/polymerizations were performed in a 250 mL glass reactor equipped with a septum adapter and a magnetic stir bar. The required amount of catalyst was added to the reactor and kept under vacuum for 30 min and then purged with N_2. The reactor was then charged with toluene (80 mL) under N_2 and then pressurized with ethylene (1.3 bar) at the desired temperature with stirring. The polymerization was started by the addition of cocatalyst. The ethylene flow to the reactor was monitored by a mass flow meter from the rate of consumption, measured by a hotwire flow meter (model 5850 D from Brooks Instrument Div.) connected to a personal computer through an A/D converter. After the given reaction time, for polymerization, the reaction was quenched by the addition of acidified methanol followed by precipitation in methanol. The polymer was then washed several times with methanol and dried in a vacuum oven to constant weight. For oligomerizations, the samples are collected from the reactor for analysis and passed through a silica column to remove catalyst and are analyzed by gas chromatography. The oligomerization rate was determined from a mass flow meter connected to the computer.

■ ASSOCIATED CONTENT

Supporting Information. Structure refinement and CIF files containing X-ray diffraction data of complexes **5** and **10** and synthesis of compound **2** are available free of charge via the Internet at http://pubs.acs.org.

■ AUTHOR INFORMATION

Corresponding Author

*E-mail: ilkim@pusan.ac.kr. Tel: +82-51-510-2399. Fax: +82-51-513-7720.

■ ACKNOWLEDGMENT

The authors thank H. J. Lee of KBSI, Jeonju Center, and J. E. Lee of Central Instrumentation Facility, Gyeongsang National University, for assistance with X-ray crystallographic analysis. This work was financially supported by the World Class University Program (No. R32-2008-000-10174-0). The authors are also grateful to the National Core Research Center Program from MEST and KOSEF (R15-2006-022-01002-0).

■ REFERENCES

(1) Galli, P.; Vecellio, G. J. *J. Polym. Sci. A: Polym. Chem.* **2004**, *42*, 396.
(2) Vogt, D. In *Applied Homogeneous Catalysis with Organometallic Compounds*; Cornils, B; Herrmann, W. A., Eds.; VHC: New York, 1996; Vol. 1, p 245.
(3) Skupinska, J. *Chem. Rev.* **1991**, *91*, 613.
(4) Parshall, G. V.; Ittel, S. D. Homogeneous Catalysis. In *The Applications and Chemistry of Catalysis by Soluble Transition Metal Complexes*; John Wiley and Sons: New York, 1992; p 68.
(5) Gibson, V. C.; Spitzmesser, S. K. *Chem. Rev.* **2003**, *103*, 283.
(6) Britovsek, G. J. P.; Gibson, V. C.; Wass, D. F. *Angew. Chem., Int. Ed.* **1999**, *38*, 428.
(7) Ittel, S. D.; Johnson, L. K.; Brookhart, M. *Chem. Rev.* **2000**, *100*, 1169.
(8) Mecking, S. *Angew. Chem., Int. Ed.* **2001**, *40*, 534.
(9) Park, S.; Han, Y.; Kim, S. K.; Lee, J.; Kim, H. K.; Do, Y. *J. Organomet. Chem.* **2004**, *689*, 4263.
(10) Small, B. L.; Brookhart, M.; Bennett, A. M. A. *J. Am. Chem. Soc.* **1998**, *120*, 4049.
(11) Small, B. L.; Brookhart, M. *J. Am. Chem. Soc.* **1998**, *120*, 7143.
(12) Gibson, V. C.; Britovsek, C. J.; Kimberley, B. S.; Maddox, P. J.; Maddox, P. J.; McTavish, S. J.; Solan, G. A.; White, A. J. P.; Williams, D. J. *Chem. Commun.* **1998**, 849.
(13) Britovsek, G. J. P.; Bruce, M.; Gibson, V. C.; Kimberley, B. S.; Maddox, P. J.; Mastroianni, S.; McTavish, S. J.; Redshaw, C.; Solan, G. A.; Stromberg, S.; White, A. J. P.; Williams, D. J. *J. Am. Chem. Soc.* **1999**, *121*, 8728.
(14) Britovsek, G. J. P.; Mastroianni, S.; Solan, G. A.; Baugh, S. P. D.; Redshaw, C.; Gibson, V. C.; White, A. J. P.; Williams, D. J.; Elsegood, M. R. J. *Chem.—Eur. J.* **2000**, *6*, 2221.
(15) Bianchini, C.; Giambastiani, G.; Rios, I. G.; Mantovani, G.; Meli, A.; Segarra, A. M. *Coord. Chem. Rev.* **2006**, *250*, 1391.
(16) Gibson, V. C.; Redshaw, C.; Solan, G. A. *Chem. Rev.* **2007**, *107*, 1745.
(17) Sun, W.-H.; Zhang, S.; Zuo, W. *C. R. Chimie* **2008**, *11*, 307.
(18) Britovsek, G. J. P.; Baugh, S. P. D.; Hoarau, O. D.; Gibson, V. C.; Wass, D. F.; White, A. J. P.; Williams, D. J. *Inorg. Chim. Acta* **2003**, *345*, 279.
(19) Small, B. L.; Rios, R.; Fernandez, E. R.; Carney, M. J. *Organometallics* **2007**, *26*, 1744.
(20) Britovsek, G. J. P.; Gibson, V. C.; Hoarau, O. D.; Spitzmesser, S. K.; White, A. J. P.; Williams, D. J. *Inorg. Chem.* **2003**, *42*, 3454.
(21) Britovsek, G. J. P.; Gibson, V. C.; Kimberley, B. S.; Mastroiannni, S.; Redshaw, C.; Solan, G. A.; White, A. J. P.; Williams, D. J. *J. Chem. Soc., Dalton Trans.* **2001**, 1639.
(22) Jie, S.; Zhang, S.; Sun, W.-H.; Kuang, X.; Liu, T.; Guo, J. *J. Mol. Catal. A: Chem.* **2007**, *269*, 85.
(23) Zhang, M.; Hao, P.; Zuo, W.; Jie, S.; Sun, W.-H. *J. Organomet. Chem.* **2008**, *693*, 483.
(24) Zhang, M.; Gao, R.; Hao, X.; Sun, W.-H. *J. Organomet. Chem.* **2008**, *693*, 3867.
(25) Sun, W.-H.; Hao, P.; Li, G.; Zhang, S.; Wang, W.; Yi, J.; Asma, M.; Tang, N. *J. Organomet. Chem.* **2007**, *692*, 4506.
(26) Sun, W.-H.; Hao, P.; Zhang, S.; Shi, Q.; Zuo, W.; Tang, X.; Lu, X. *Organometallics* **2007**, *26*, 2720.
(27) Wang, K.; Wedeking, K.; Zuo, W.; Zhang, D.; Sun, W.-H. *J. Organomet. Chem.* **2008**, *693*, 1073.
(28) Zhang, S.; Vystorop, I.; Tang, Z.; Sun, W.-H. *Organometallics* **2007**, *26*, 2456.
(29) Davies, C. J.; Fawcett, J.; Shutt, R.; Solan, G. A. *Dalton Trans.* **2005**, 2630.
(30) Bianchini, C.; Mantovani, G.; Meli, A.; Migliacci, F.; Laschi, F. *Organometallics* **2003**, *22*, 2545.
(31) Xiao, L.; Gao, R.; Zhang, M.; Li, Y.; Cao, X.; Sun, W.-H. *Organometallics* **2009**, *28*, 2225.
(32) Zhang, S; Sun, W.-H.; Xiao, T.; Hao, X. *Organometallics* **2010**, *29*, 1168.
(33) Bianchini, C.; Giambastiani, G.; Rios, I. G.; Meli, A.; Passaglia, E.; Gragnoli, T. *Organometallics* **2004**, *23*, 6087.
(34) Esteruelas, M. A.; López, A. M.; Méndez, L.; Oliván, M.; Oñ ate, E. *Organometallics* **2003**, *22*, 395.

(35) Smit, T. M.; Tomov, A. K.; Gibson, V. C.; White, A. J. P.; Williams, D. J. *Inorg. Chem.* **2004**, *43*, 6511.
(36) Thummel, R. P.; Jahng, Y. *J. Org. Chem.* **1985**, *50*, 2407.
(37) Archer, A. M; Bouwkamp, M. W.; Cortez, M.-P.; Lobkovsky, E.; Chirik, P. J. *Organometallics* **2006**, *25*, 4269.
(38) Sun, W.-H.; Wang, K.; Wedeking, K.; Zhang, D.; Zhang, S.; Cai, J.; Li, Y. *Organometallics* **2007**, *26*, 4781.
(39) Chen, Y.; Chen, R.; Qian, C.; Dong, X.; Sun, J. *Organometallics* **2003**, *22*, 4312.
(40) Flory, P. J. *J. Am. Chem. Soc.* **1940**, *62*, 1561.
(41) Schulz, G. V. Z. *Phys. Chem. Abt. B* **1935**, *30*, 379.
(42) Schulz, G. V. Z. *Phys. Chem. Abt. B* **1939**, *43*, 25.
(43) Meurs, M. V.; Britovsek, G. J. P.; Gibson, V. C.; Cohen, S. A. *J. Am. Chem. Soc.* **2005**, *127*, 9913.
(44) Britovsek, G. J. P.; Cohen, S. A.; Gibson, V. C.; Meurs, M. V. *J. Am. Chem. Soc.* **2004**, *126*, 10701.
(45) Tomov, A. K.; Gibson, V. C.; Britovsek, G. J. P.; Long, R. L.; Meurs, M.; Jones, D. J.; Tellmann, K. P.; Chirinos, J. J. *Organometallics* **2009**, *28*, 7033.